RSC Advances

Nd-Containing Coordination Ploymer: Syntheses, Crystal Structure and Application as A Nucleating Agent for Isotactic Polypropylene

RSC Advances

ARTICLE

Nd-Containing Coordination Ploymer: Syntheses, Crystal Structure and Application as A Nucleating Agent for Isotactic Polypropylene†

Wei Qian,[a] Jiaqi Wang,[a] Shudong Liu,[a] Shaohui Guo,*[a] Yongjun Lu,[b] Hui Lin,[a] De Zheng[b]

A novel Nd coordination ploymer [Nd(N-phgly)(Pha)(H$_2$O)](H$_2$O)$_2$ has been solvothermally synthesized and characterized crystallographically. It is a novel 3D framework supramolecular structure coordination polymer that contains two different carboxylate liqands N-phthaloylglycine (N-phgly) and phthalic acid (Pha). The complex was characterized by elemental analysis, FT-IR spectra, X-ray single-crystal diffraction, thermal gravimetric analyzer and the powder XRD. It was incorporated into isotactic polypropylene (iPP). Then, the performance, non-isothermal crystallization behaviors, crystalline morphologies and optical properties of modified iPP were evaluated and studied. These results show that the complex is an effective and novel nucleating agent. It results in an increase in the overall crystallization rate and a decrease in the spherulite size of iPP. The Izod impact strength of NA-iPP is higher than the pure iPP. The addition of it makes the stiffness and impact resistance of iPP improve obviously. Meanwhile, the nucleated iPP displays a good balance between toughness and stiffness. Besides, the optical characteristics are also improved.

Introduction

Polypropylene (PP) is a very significant general-purpose engineering thermoplastic material. Compared with other engineering plastics, PP is one kind of semicrystalline polymer. For semicrystalline polymers, the crystalline morphological and other microstructural characteristics can have a dramatic effect on macro-properties.[1-4] The macro-properties is important to engineering application. Thus, semicrystalline polymer, isotactic polypropylene (iPP) presents poor mechanical properties (impact strength, tensile strength, flexural modulus and bending strength) and cannot meet the high requirements in strength and stiffness for engineering applications. Isotactic polypropylene shows obvious polymerisms and morphologies, which exist in several crystal modifications with monoclinic (α), trigonal (β), orthorhombic (γ) and smectic.[5-11] The α-monoclinic form is the most prevalent and stable modification. In general it is the thermodynamically stable one and principal phase, which can generate in iPP under ordinary processing conditions. The crystallisation of iPP is controlled by the nucleation stage. In the application of engineering, the crystallization of iPP is usually speeded up with nucleating agents. These nucleating agents reduce the induction time of crystallization and increase the crystallization rate by accelerating the formation of nuclei for crystal growth. More nucleation sites result in an increase in the overall crystallization rate and a decrease in the spherulite size.[5, 12-16] The changes of microstructural characteristics cause the mechanical properties and thermal stability of iPP to be improved. The addition of specific nucleating agents can also shorten injection-moulding cycle times.[16, 17] Thus, it can obviously reduce production costs. The α-nucleating agents can induce more α phase and increase the crystallization rate. Furthermore, such agents generate smaller spherulites and improve the mechanical and optical properties.[18-20] Generally, the properties of stiffness and toughness are contradictions. So far, many compounds have been synthesized as nucleating agents for α form of iPP. They have common characteristics that the Izod impact strength is deteriorated and the blending strength is increased.[20-22]

By the following work, the author wish the lanthanide coordination polymers could display different functions in iPP. Because rare earths have unique features and have hardly been used in polypropylene.

During the last two more decades, lanthanide coordination polymers have received extensive attention for their amazing potential applications in magnetism,[23-30] catalysis,[31-35] sensors,[36-40] gas storage and absorption,[41-45] and luminescent materials,[23, 26, 28-30, 46, 47] etc. Meanwhile, the study of lanthanide carboxylic acids complexes is an active field

a. State Key Laboratory of Heavy Oil Processing, Beijing Key Laboratory of Oil and Gas Pollution Control, China University of Petroleum, Beijing, 18 Fuxue Road, Changping District, Beijing 102249, P. R. China. E-mail: cupgsh@163.com
b. Guangdong Winner New Materials Technology Co., Ltd, Foshan 528521, P. R. China.
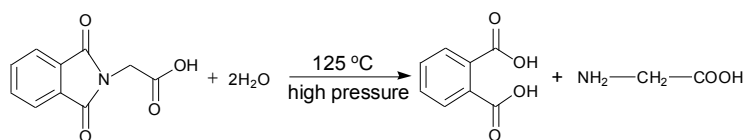
Scheme 1   In situ solvothermal N-phgly was unexpectedly partially decomposed to phthalic acid

because of their changeable coordination modes and fascinating properties. Among the metal carboxylic acids complexes, the metal complexes of aromatic carboxylic acids have higher stability. Furthermore, N-phthaloylglycine (N-phgly), a significant N-protected amino acid, and its derivatives have been widely applied, because they are intermediates in the synthesis of various metal complexes, which presents amazing biological and medical functions.[48-50] So far, only a few metal coordination ploymers containing N-phgly and its derivatives were reported and synthesized using the conventional solution method.[51, 52] N-phgly contains imide groups. Moreover, some nucleating agents of polypropylene involve imide groups.[53] In addition, the Nd(III) ion has special configuration of $4f^3$ electrons and the nucleating agent for polypropylene should be light-colored, otherwise it may affect the color of the appearance of the finished products.

Based on the abovementioned consideration, a novel Nd coordination ploymer [Nd(N-phgly)(Pha)(H_2O)](H_2O)_2 has been solvothermally synthesized and characterized crystallographically. It contains two different carboxylate liqands N-phgly and phthalic acid. Interestingly, the reaction material didn't have phthalic acid, but the product contained it. In situ solvothermal N-phgly was unexpectedly partially decomposed to phthalic acid (Scheme 1). It was added into iPP, then the effects of the complex were investigated with DSC, and polarized optical microscope. Meanwhile, mechanical performance, heat resistance performance, optical properties of the nucleated iPP were also evaluated.

Experimental

Materials and methods

All the materials were purchased and used as received without further purification (see ESI†). Elemental analyses (C, H, and N) were tested on a Elementar instrument Vario EL cube elemental analyzer, while Nd(III) was determined by titration with EDTA using xylenol orange as the indicator. IR spectra (KBr) data was generated on a Bruker Tensor27 FT-IR Spectrometer within the 4000-400 cm^{-1} region. The crystal structure data of the complex was obtained on a Bruker Smart 1000 CCD X-ray single crystal diffractometer using Mo-Kα radiation (λ = 0.7107 Å). The powder XRD data was collected on a Empyrean X-ray diffractometer using Mo-Kα radiation (λ = 0.7107 Å). Thermogravimetric analysis (TGA) experiment of the coordination ploymer was carried out on a Netzsch TG209F3 instrument with a heating rate of 20 ^{o}C min^{-1} in the range of 35-900 ^{o}C under a N_2 atmosphere. A series of compositions with different content (the additive concentration of NA range from 0 to 0.5 wt%.) of [Nd(N-phgly)(Pha)(H_2O)](H_2O)_2 (NA) in iPP were prepared by melt blending in a co-rotating twin screw

extrude. The composition with 0.15 wt% TMP-5 (a stiffening nucleating agent) in iPP was prepared by the same method for comparison. The extruded pellets of different series and neat iPP pellets were injection-molded into test samples using an injection molding machine, respectively. The test specimens were prepared for studying the performance changes of iPP. The performance contains bending strength, notched Izod impact strength, tensile strength, heat deflection temperature (HDT), haze and clarity. The specimens for DSC were prepared by compression molding into 1 mm thick sheets at 210 ^{o}C. A differential scanning calorimetry (Perkin Elmer Jade DSC) with nitrogen as purge (30 mL min^{-1}) was used to study the non-isothermal crystallization behaviors of these samples. Crystalline morphologies of some selected samples were observed by using an Leica DM2500 P polarized optical microscope with a THMS 600 hot-stage attached. The detailed information of samples preparation is shown in ESI†.

Synthesis of [Nd(N-phgly)(Pha)(H_2O)](H_2O)_2

A mixture of N-phgly (15.465 g, 75 mmol), Nd(NO_3)_3·6H_2O (10.957 g, 25 mmol), H_2O/CH_3OH (80 mL, v/v, 7/1), NaOH (3.003 g, 75 mmol) was heated to 125 ^{o}C for 72 hours in an 800 mL hydrothermal reaction vessel. Light prism block crystals were collected by filtration, washed with pure water and ethanol, and dried in air.

[Nd(N-phgly)(Pha)(H_2O)](H_2O)_2 (**1**). Yield: 7.564g, 53.4% (based on Nd) (Fw=566.56). Anal. calcd for **1** (C_18H_16NdNO_11): C, 38.12; H, 2.91; N, 2.39; Nd, 25.82; Found: C, 38.16; H, 2.85; N, 2.47; Nd, 25.46%. IR (cm^{-1}): 3462 (s), 3051 (w), 1756 (s), 1711 (s), 1619 (s), 1539 (s), 1425 (s), 1386 (s), 1286 (s), 1115(s), 962 (s), 742 (s), 702 (s).

SXRD detials and structure refinement

The X-ray intensity data of the complex **1** was collected on a Bruker Smart 1000 CCD X-ray single crystal diffractometer using Mo-Kα radiation (λ = 0.7107 Å) at 150 K. An empirical absorption correction was applied via the multi-scan technique. The intensity data was corrected for Lorentz, polarization and absorption effects. In all the cases, the highest possible space group was selected. The structure was solved by the direct method and refined by full-matrix least-squares fitting on F^2 using SHELX-97.[54] The non-hydrogen atoms were all refined anisotropically. The hydrogen atoms were fixed at calculated positions and refined as riding atoms except water molecules. The hydrogen atoms of water were refined by the use of geometrical restraints. Table 1 shows the crystallographic data collection and refinement parameters of complex **1**. Table S-1 presents the selected bond distances and angles (ESI†).

Table 1 Crystal Data and Structure Refinement for complex **1**

Empirical formula	$C_{18}H_{16}NdNO_{11}$
Fw	566.56
Crystal system	Monoclinic
Space group	$P2_1/c$
a (Å)	14.6950(4)
b (Å)	7.1251(2)
c (Å)	19.3703(4)
α (deg)	90.00
β (deg)	108.558(3)
γ (deg)	90.00
Z	4
V (Å^3)	1922.68(9)
ρ_{calc} (g cm^{-3})	1.957
μ (mm^{-1})	2.766
F(000)	1116.0
Final R indices [$I > 2\sigma(I)$]	R_1=0.0225, wR_2=0.0489
Final R indices (all data)	R_1=0.0275, wR_2=0.0507
GOF on F^2	1.047
$\Delta\rho_{max}$, $\Delta\rho_{min}$ (e Å^{-3})	1.064, -0.759
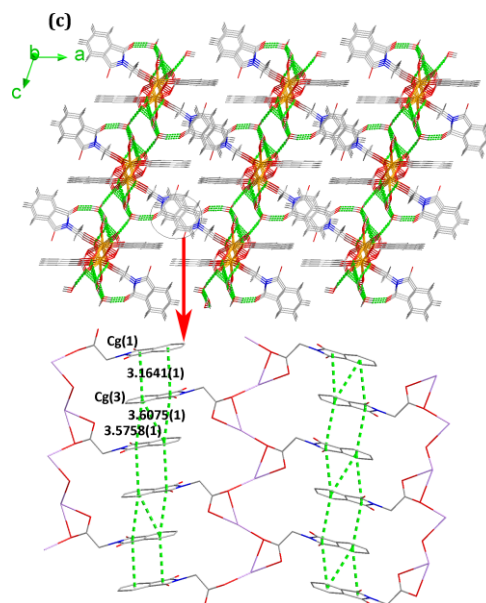
Fig.1 (a) Coordination environment of the Nd atom in **1**. Symmetry codes: A, -x+1,y+1/2,-z+1/2; B, -x+1,y-1/2,-z+1/2. (b) The 2D supramolecular layer and the H-bonds interactions network of **1**. (c) Packing diagram of **1** with the dashed lines representing H-bonds and π-π stacking interactions.
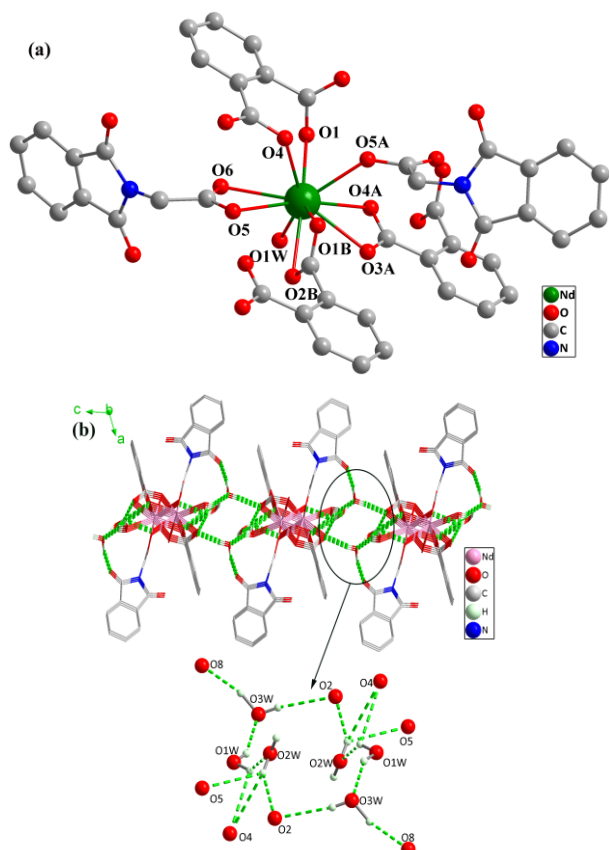
Results and discussion

Description of the crystal structure

Complex **1** crystallizes in the monoclinic space group $P2_1/c$. As shown in Fig.1(a), the asymmetric unit contains one Nd(III) ion, one deprotonic N-phgly ligand, one deprotonic phthalic acid ligand, two lattice water molecules and one coordinated water molecule. The two lattice water molecules are not shown in the Fig.1(a) for the sake of simplicity. The picture shows the Nd^{3+} ion is ten-coordination by three oxygen atoms (O5, O6 and O5A) from two different N-phgly ligands, six oxygen atoms (O1, O4, O3A, O4A, O1B and O2B) from three different phthalic acid ligands and one oxygen atom (O1W) from the coordinated water molecule, and presents a distorted biscapped square antiprism coordination geometry. The Nd-O bond distances range from 2.402(2) Å to 2.828(2) Å and these bond distances correspond with the previously reported Nd-$O_{carboxylate}$ bond lengths.[55-57] For complex **1**, the carboxyl group of N-phgly ligand adopts the bridging tridentate μ_2-η^2:η^1 coordination mode between two adjacent Nd(III) ions. In addition, two carboxyl groups of phthalic acid both acts as the bridging tridentate μ_3-η^2:η^2:η^2 coordination mode[58, 59] among three adjacent Nd(III) ions, which were reported in some metal complexes.[60-62] Fig.S1(a)† shows the coordination modes of complex **1** in detail.

Complex **1** shows 1D infinite O-Nd-O chains along the b-axis via Nd atoms and the oxygen atoms of N-phgly and phthalic acid ligands (Fig.S1(b)†). The 1D infinite chains are linked via

the coordinated water, the oxygen atoms (O2, O4, O5 and O8) of carboxylate ligands and the isolated water molecules. The H-bonds lengths and angles are shown in Table S-2†. The H-bonds are shown in Fig.1(b). Fig.1(c) is the packing dragram of complex **1** with the dashed lines representing H-bonds and π-π stacking interactions. Plane Cg(1) is composed of five atoms (N1, C9, C10, C15 and C16). Plane Cg(3) is composed of C atoms from C10 to C15. The dihedral angle between plane Cg(1) and plane Cg(3) is only 1°. The distance between ring centroids Cg(1) and Cg(3) is about 3.6141(1) Å or 3.5758(1) Å. Cg(3) and Cg(3) of adjacent layers are slipped stacked arrangement. The distance between Cg(3) and Cg(3) is about 3.6075(1) Å or 4.3746(1) Å. The π-π stacking interaction s can be ignored, when the distance between Cg(3) and Cg(3) is 4.3746(1) Å.[63, 64] The π-π stacking interactions relate to the stacked direction and position of ligands of N-phgly. The H-bonds and π-π stacking interactions play significant roles in the formation of stable 3D framework supramolecular structure. The π-π stacking interations detailed data of complex **1** is given in Table S-3†.

IR Spectra, Thermogravimetric Analyses (TGA) and X-ray powder diffraction analyses for complex 1

The IR spectrum and experimental powder XRD analyses for complex **1** are shown in Fig.S2 and S3†, respectively. The experimental powder XRD pattern is almost consistent with the simulated one, indicating complex **1** is isostructural and crystalline phase. To study thermal stability of complex **1**, TGA were performed from 35 ^{o}C to 900 ^{o}C with a heating rate of 20 ^{o}C min^{-1} under a N$_2$ atmosphere. The TGA curve of complex **1** indicates a weight loss of 9.0% from 30 ^{o}C to 220 ^{o}C, which is consistent with one coordinated water molecule and two isolated water molecules (calcd: 9.5%). A constant stage is observed till 330 ^{o}C. Beyond 330 ^{o}C, the complex starts to decompose rapidly. Namely, the organic ligands begin to decompose (Fig. S4†).

Mechanical properties

NA-iPP represents the iPP with a certain content of complex **1**. The mechanical properties were measured according to ATSM test methods (ESI†). The values of all the mechanical properties were calculated as averages of over five samples. Fig.2(a) and (b) illustrate changes in flexural modulus, bending strength and tensile strength of NA-iPP. When the concentration of NA (complex **1**) is 0.15 wt%, compared to those properties of pure iPP, the flexural modulus, bending strength and tensile strength of iPP are increased by 31.5%, 21.8% and 13.6%, respectively. These changes indicate NA has an obvious nucleation effect on iPP. The following descriptions can explain these results. Firstly, the α-iPP shows a lamellar branching. The branching results in both nearly and radial tangential orientation of lamellae in spherulites growth. This is an intrinsic property of α-iPP. The microstructure of iPP determines macroscopic mechanical properties. Furthermore, the α-nucleating agent (NA) leads iPP to generate more and smaller α form spherulites. NA belongs to the same crystal system with the α phase of iPP, namely, monoclinic crystal
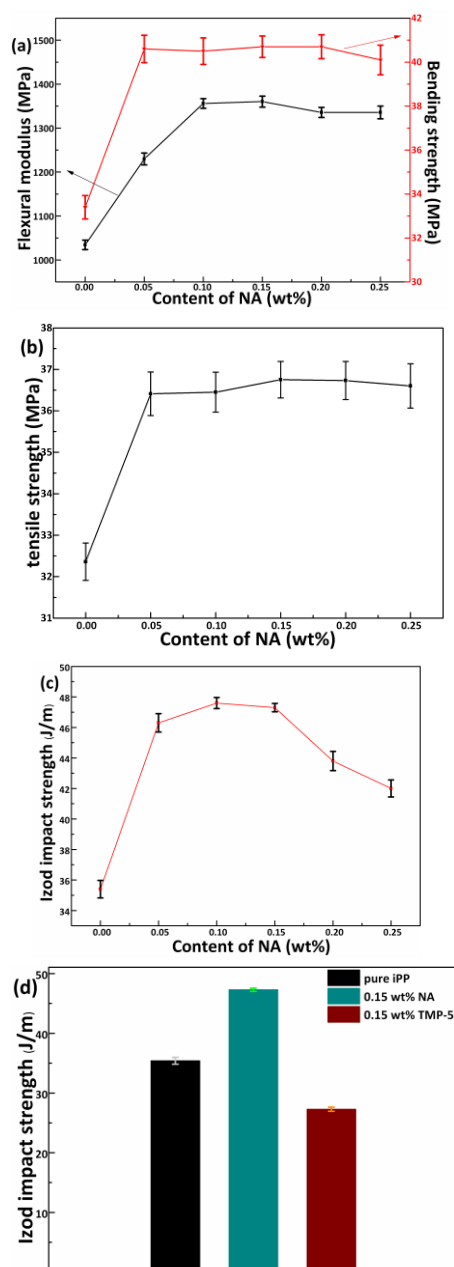
Fig.2 (a) Effect of α-nucleating agent on flexural modulus and bending strength of iPP. (b) Effect of α-nucleating agent on tensile strength of iPP. (c) Effect of α-nucleating agent on Izod impact strength of iPP. (d) Effect of 0.15 wt% NA and 0.15 wt% TMP-5 on Izod impact strength of iPP.

system. Therefore, NA can induce more α phase and increase crystallization rate. Thus, stiffness of α-iPP is improved by the addition of α-nucleating agent (namely, NA). Excessive concentration of NA can lead the flexural modulus to decrease, but the flexural modulus is still higher than that of virgin iPP. The optimum concentration of NA is 0.15 wt%. There are no more good changes on iPP mechanical properties when the content of nucleating agent is more than 0.15 wt%. Because overmuch heterogeneous nucleation can lead to a little powder of nucleating agent get together, and the crystallite shape of iPP becomes imperfect.

Interestingly, when the concentration of NA is 0.15 wt%, the Izod impact strength increases from 35.4 J m^{-1} to 47.3 J m^{-1}, compared to that of pure iPP (Fig.2(c)). The situation has hardly been observed before, when the addition is a α-nucleating agent. Because the overall crystallization rate is increase and more smaller spherulites. In addition, this may be owing to its unique properties (such as, special configuration of 4f^3 electrons) of neodymium and imide group of N-phgly ligand's function. Imide group may generate H-bonds and other intermolecular interactions with -CH2 or -CH3 groups of iPP. So, iPP can resist more impact energy. To sustain this opinion, the iPP samples with 0.15 wt% TMP-5 (a stiffening nucleating agent) are tested for comparison. Fig.2(d) shows the changes on Izod impact strength. When the concentration of TMP-5 is 0.15 wt%, the Izod impact strength decreases from 35.4 J m^{-1} to 27.3 J m^{-1}, compared to that of pure iPP. So, NA-iPP exhibits better impact resistance than TMP-5-iPP and pure iPP. The changes of nucleated iPP on flexural modulus and bending strength are shown in Fig. S5†.

In a word, NA can improve both the rigidity and toughness of nucleated iPP. This is infrequent, while the iPP matrix only incorporates into a α-nucleating agent.

Heat deflection temperature (HDT)

With 0.15 wt% NA incorporated into iPP, the heat deflection temperature (HDT) of iPP increases from 79.9 ^{o}C to 104.5 ^{o}C. This means NA has a stronger nucleating ability (Table S-4†). The result is corresponding with the conclusions of mechanical tests.

Non-isothermal crystallization behaviors

For studying the nucleation effect of NA, these samples were heated from 50 ^{o}C to 210 ^{o}C at a standard rate of 10 ^{o}C min^{-1} and maintained at 210 ^{o}C for 5 min to eliminate their thermal history. Then, the non-isothermal crystallization process of the test bars was measured by cooling samples from 210 ^{o}C to 50 ^{o}C at the same standard rate of 10 ^{o}C min^{-1}. A heating rate of 10 ^{o}C min^{-1} was then run from 50 ^{o}C to 210 ^{o}C to obtain the melting behaviors of these samples. As shown in Fig.3(a), the onset crystallization temperature (T$_o$) and crystallization peak temperature (T$_p$) of pure iPP are about 127.9 ^{o}C and 109.2 ^{o}C, respectively. While, the addition of NA improves T$_o$ from 127.9 ^{o}C (pure iPP) to 131.9 ^{o}C (0.15 wt% NA) and T$_p$ from 109.2 ^{o}C (pure iPP) to 122.9 ^{o}C (0.15 wt% NA). Additionally, the crystallization rate of non-isothermal crystallization process is also different. The relative crystallinity, X(T), is calculated by the following equation[65, 66]:

$$X(T) = \frac{\int_{T_o}^{T}(\frac{dH}{dt})dt}{\int_{T_o}^{T_e}(\frac{dH}{dt})dt} \times 100\% \quad (1)$$

where (dH/dt) is the heat-evolution rate; T$_o$ and T$_e$ are the onset and end of crystallization temperatures, respectively. The X(T)-T curve can be presented by the following method. Using t=(T$_o$-T)/k (where k is the cooling rate, T is the
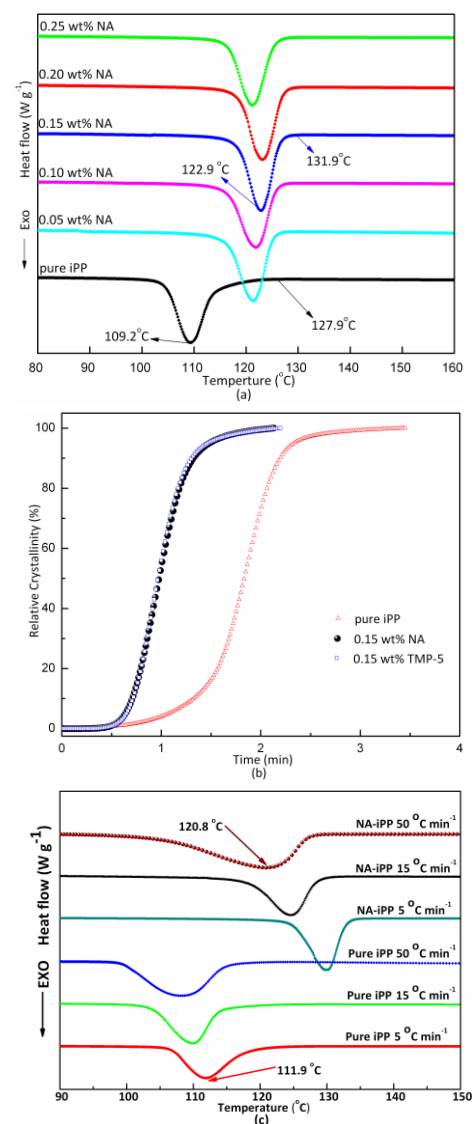
Fig.3 (a) DSC cooling curves of NA-iPP samples after erasing the thermal history. (b) Polts of relative crystallinity (X(T)) vs. crystallization time for pure iPP, 0.15 wt% NA-iPP and 0.15 wt% TMP-5-iPP. (c) DSC cooling curves of neat iPP and NA-iPP (0.15 wt% NA) samples with different cooling rates.

temperature at crystallization time, t). Thus, the X(T)-T curve can be transformed into X(t)-t curve. The relative crystallinity (pure iPP, 0.15 wt% NA, 0.15 wt% TMP-5) of X(t)-t curve is shown in Fig.3(b). Fig.S6† indicates NA can improve the melting peak temperature of iPP slightly. Fig.3(a), (b) and Fig.S6 all indicate that NA is an efficient α-nucleating agent and accelerating crystallization process of matrix, which is in agreement with the above results. In other words, NA can increase crystallization rate and reduce the time of crystallization.

In order to study the influence of different cooling rates on the crystallization temperature peak, the samples of neat iPP and iPP with 0.15 wt% NA were measured by different cooling rates (5 ^{o}C min^{-1}, 15 ^{o}C min^{-1} and 50 ^{o}C min^{-1}) after erasing the

thermal history. In the Fig.3(c), obviously, the increase of cooling rate makes the crystallization peaks of the materials become wider and move toward lower temperature. When the cooling rate is 5 ^{o}C min^{-1}, the crystallization peak temperature of neat iPP is only 111.9 ^{o}C. However, when the cooling rate is 50 ^{o}C min^{-1}, the crystallinzation peak temperature of NA-iPP is still 120.8 ^{o}C. It suggests that these additives (such as, catalyst residues and stabilizers) of neat iPP have no influence on the nucleation efficiency at different cooling rates. Therefore, NA is an efficient nucleating agent. Thus, it can shorten the processing cycle and reduce costs for industrial production.

Crystalline morphology

The melting and crystallization behaviour of different samples (pure iPP, iPP with 0.15 wt% NA) crystallized at different cooling rates. The samples were investigated from the melt to room temperature at cooling rates of 20 ^{o}C min^{-1} and 50 ^{o}C min^{-1}. The optical micrographs are shown in Fig.4(a), (b), (c) and (d), respectively. As shown in the TGA curve (Fig.S4†) and Fig.4, NA cannot melt under the processing temperature of iPP and a solid phase (namely, NA, [Nd(N-phgly)(Pha)(H$_2$O)](H$_2$O)$_2$) always exists. The composites (NA-iPP) are an immiscibility binary system. This is different from the reported binary system, iPP and nucleating agents.[67, 68] These figures suggest the iPP is epitaxial crystallization via the solid phase (namely, NA, [Nd(N-phgly)(Pha)(H$_2$O)](H$_2$O)$_2$) in the immiscibility binary system. NA belongs to the same crystal system with the α phase of iPP, namely, monoclinic crystal system. Therefore, NA can induce more α phase and increase crystallization rate. As shown in Fig. 5, the noticeable nucleating effect of NA on iPP is observed.
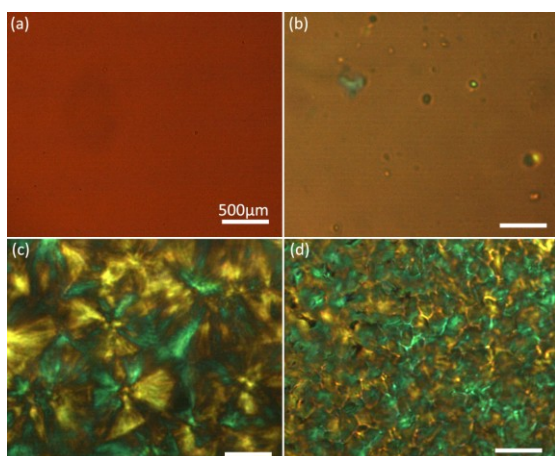
Fig.4   The polarized optical micrograph of iPP at different cooling rates (scale bar: 500μm) (a) pure iPP (cooling rate: 20 ^{o}C min^{-1}, picture taken at 250 ^{o}C); (b) iPP with 0.15wt% NA (cooling rate: 20 ^{o}C min^{-1}, picture taken at 250 ^{o}C); (c) pure iPP (cooling rate: 50 ^{o}C min^{-1}, picture taken at 110 ^{o}C); (d) iPP with 0.15wt% NA (cooling rate: 20 ^{o}C min^{-1}, picture taken at 125 ^{o}C)
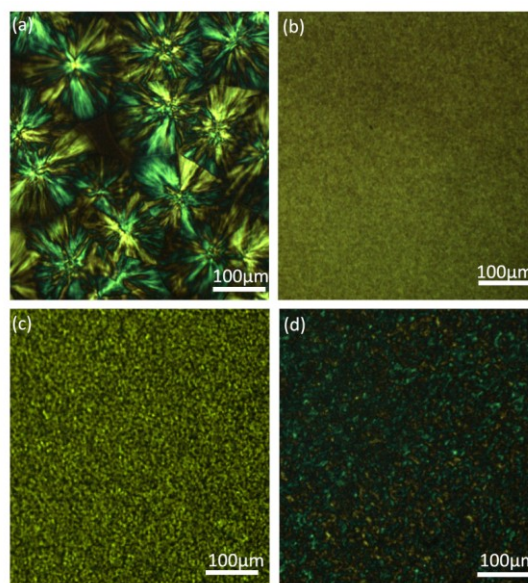
Fig.5 The polarized optical micrograph of iPP at different cooling rates (Scale bar: 100μm) (a) pure iPP (cooling rate: 50°C min^{-1}, picture taken at 107 ^{o}C); (b) iPP with 0.15wt% NA (cooling rate: 5 ^{o}C min^{-1}, picture taken at 129 ^{o}C); (c) iPP with 0.15wt% NA (cooling rate: 20 ^{o}C min^{-1}, picture taken at 125 ^{o}C); (d) iPP with 0.15wt% NA (cooling rate: 50 ^{o}C min^{-1}, picture taken at 118 ^{o}C).

With the increasing of cooling rate (From 5 ^{o}C min^{-1} to 50 ^{o}C min^{-1}), the crystallization temperature is decreased. From these pictures, we can know NA decreases the spherulite size of iPP remarkably. Moreover, the crystallization temperatures are all higher than pure iPP. The overall crystallization rate of iPP is decided by both the rate of crystal growth and the rate of crystal nucleation. Nuclei can hardly form in pure iPP. In pure iPP, the growth of spherulite is mainly homogeneous nucleation. Then, homogeneous crystal nucleus control spherulite growth. However, the number of nucleus is very few and nucleation rate is slow in pure iPP. Thus, the spherulite size of iPP becomes very large before it can touch another crystal nuclei (Fig.5(a),(c)). While NA is incorporated into iPP, many heterogeneous nucleus can be generated and so the nucleation rate is very quick. As shown in Fig.5(b), (c) and (d), a large number of heterogeneous nucleus make the iPP spherulites cannot grow big enough before overlapping. Thus, the size of iPP spherulites can be smaller than those in pure iPP. This means NA is effective in nucleation activity.

Optical properties

The optical characteristics haze and clarity of injection-molded NA-iPP samples (ESI†) were measured in the additive concentration of NA range from 0 to 0.5 wt%. In this test, clarity refers to the scattering contribution at small angles (θ <

Journal Name ARTICLE
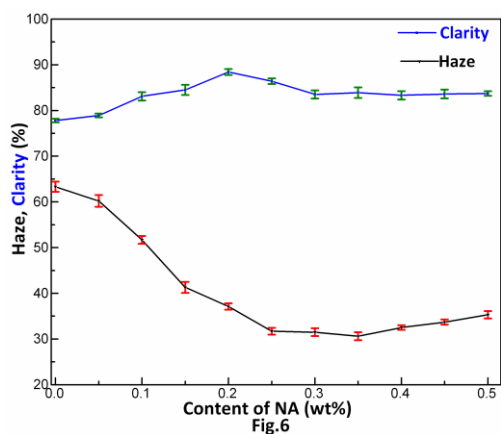
Fig.6 Clarity and haze of injection-molded samples of NA-iPP as function of the content of NA.

2.5 ^{o}) and is related to the sharpness of an object when viewed through the sample. Haze is commonly defined as that portion of visible light that is scattered at wider angles (2.5 ^{o}< θ < 90 ^{o}) and is a measure for the turbidity of a sample.[67] As shown in Fig.6, with the increase of content of NA, these optical characteristics were improved. When the concentration of the nucleating agent (NA) is 0.15 wt%, the addition of NA increase the clarity of iPP by 9.9%. In contrast, the haze of iPP is reduced by 34.1%. When the concentration of NA is around 0.35 wt%, the haze of iPP has the minimum value. When the concentration of NA is around 0.2 wt%, the clarity of iPP has the maximum value. From abovementioned results, we can know the addition of NA causes a decrease in the spherulite size. The small spherulite is benefical to improve the optical properties.

Conclusions

In this work, a novel 3D framework supramolecular structure coordination polymer [Nd(N-phgly)(Pha)(H$_2$O)](H$_2$O)$_2$ was synthesized under solvothermal conditions. When it was incorporated into iPP, it revealed a strong heterogeneous nucleating effect on iPP matrix. Interestingly, when 0.15 wt% of [Nd(N-phgly)(Pha)(H$_2$O)](H$_2$O)$_2$ was added into iPP, the Izod impact strength was remarkably increased. The other mechanical properties (the flexural modulus, bending strength and tensile strength) are also significantly improved. The situation has hardly been seen before, when the addition is a α nucleating agent (such as, fore-mentioned TMP-5).

Through the above tests (DSC, WAXD, etc.), [Nd(N-phgly)(Pha)(H$_2$O)](H$_2$O)$_2$ can improve both the rigidity and toughness of nucleated iPP. And it can also improve the optical properties of iPP. It may widen the application field of iPP. Nowadays, some researchers are actively investigating the crystallization behaviors of iPP nucleated with α/β compounding nucleating agents. Their purpose is to establish certain foundations for processing of nucleated iPP with a good balance of toughness and stiffness.[69, 70] The abovementioned results may offer a new orientation of future research for iPP.

Acknowledgements

Notes and references

1. X. Zhang and R. Cameron, *J. Appl. Polym. Sci.*, 1999, **74**, 2234-2242.
2. C. Marcó, G. Ellis, M. A. Gomez and J. M. Arribas, *J. Appl. Polym. Sci.*, 2002, **84**, 2440-2450.
3. V. Busico and R. Cipullo, *Prog. Polym. Sci.*, 2001, **26**, 443-533.
4. S. Brückner, S. V. Meille, V. Petraccone and B. Pirozzi, *Prog. Polym. Sci.*, 1991, **16**, 361-404.
5. P. Zhang, X. Liu and Y. Li, *Mater. Sci. Eng., A*, 2006, **434**, 310-313.
6. J. Wang and Q. Dou, *J. Macromol. Sci., B*, 2007, **46**, 987-1001.
7. M. Dong, Z. Guo, Z. Su and J. Yu, *J. Polym. Sci. Part B: Polym. Phys.*, 2008, **46**, 1183-1192.
8. H. Huo, S. Jiang, L. An and J. Feng, *Macromolecules*, 2004, **37**, 2478-2483.
9. C. Marcó, G. Ellis, M. A. Gómez and J. M. Arribas, *J Therm Anal Calorim*, 2002, **68**, 61-74.
10. T. Foresta, S. Piccarolo and G. Goldbeck-Wood, *Polymer*, 2001, **42**, 1167-1176.
11. B. Lotz, J. C. Wittmann and A. J. Lovinger, *Polymer*, 1996, **37**, 4979-4992.
12. B. Lotz, *Polymer*, 1998, **39**, 4561-4567.
13. J. Tang, Y. Wang, H. Liu and L. A. Belfiore, *Polymer*, 2004, **45**, 2081-2091.
14. C. L. Yin, Z. Y. Liu, W. Yang, M. B. Yang and J. M. Feng, *Colloid Polym. Sci.*, 2009, **287**, 615-620.
15. Y. f. Zhang and H. Chen, *Colloid Polym. Sci.*, 2014, **292**, 493-498.
16. Y. Huang, G. Chen, Z. Yao, H. Li and Y. Wu, *Eur. Polym. J.*, 2005, **41**, 2753-2760.
17. D. Libster, A. Aserin and N. Garti, *Polym. Advan. Technol.*, 2007, **18**, 685-695.
18. L. Balzano, G. Portale, G. W. M. Peters and S. Rastogi, *Macromolecules*, 2008, **41**, 5350-5355.
19. M. Blomenhofer, S. Ganzleben, D. Hanft, H.-W. Schmidt, M. Kristiansen, P. Smith, K. Stoll, D. Mäder and K. Hoffmann, *Macromolecules*, 2005, **38**, 3688-3695.
20. J. Wang and Q. Dou, *Polym. Int.*, 2008, **57**, 233-239.
21. Y. F. Zhang, Y. Chang, X. Li and D. Xie, *J. Macromol. Sci., B*, 2010, **50**, 266-274.
22. Z. Cai, S. Zhao, B. Shen and Z. Xin, *J. Appl. Polym. Sci.*, 2010, **116**, 792-800.
23. X. Li, H. L. Sun, X. S. Wu, X. Qiu and M. Du, *Inorg. Chem.*, 2010, **49**, 1865-1871.
24. L. Sorace, C. Benelli and D. Gatteschi, *Chem. Soc. Rev.*, 2011, **40**, 3092-3104.
25. A. Mishra, W. Wernsdorfer, K. A. Abboud and G. Christou, *J. Am. Chem. Soc.*, 2004, **126**, 15648-15649.

26. J. Yang, Q. Yue, G. D. Li, J. J. Cao, G. H. Li and J. S. Chen, *Inorg. Chem.*, 2006, **45**, 2857-2865.
27. M. Kurmoo, *Chem. Soc. Rev.*, 2009, **38**, 1353-1379.
28. J. Rocha, L. D. Carlos, F. A. A. Paz and D. Ananias, *Chem. Soc. Rev.*, 2011, **40**, 926-940.
29. J. Feng and H. Zhang, *Chem. Soc. Rev.*, 2013, **42**, 387-410.
30. C. A. Black, J. S. Costa, W. T. Fu, C. Massera, O. Roubeau, S. J. Teat, G. Aromí, P. Gamez and J. Reedijk, *Inorg. Chem.*, 2009, **48**, 1062-1068.
31. K. Mikami, M. Terada and H. Matsuzawa, *Angew. Chem. Int. Edit.*, 2002, **41**, 3554-3572.
32. P. L. Arnold, M. W. McMullon, J. Rieb and F. E. Kühn, *Angew. Chem. Int. Edit.*, 2015, **54**, 82-100.
33. P. G. Cozzi, *Chem. Soc. Rev.*, 2004, **33**, 410-421.
34. J. Inanaga, H. Furuno and T. Hayano, *Chem. rev.*, 2002, **102**, 2211-2226.
35. E. Kirillov, C. W. Lehmann, A. Razavi and J.-F. Carpentier, *J. Am. Chem. Soc.*, 2004, **126**, 12240-12241.
36. K. Miyata, Y. Konno, T. Nakanishi, A. Kobayashi, M. Kato, K. Fushimi and Y. Hasegawa, *Angew. Chem. Int. Edit.*, 2013, **52**, 6413-6416.
37. M. Schäferling, *Angew. Chem. Int. Edit.*, 2012, **51**, 3532-3554.
38. H. Tsukube and S. Shinoda, *Chem. rev.*, 2002, **102**, 2389-2404.
39. A. Balamurugan, M. L. P. Reddy and M. Jayakannan, *J. Mater. Chem. A*, 2013, **1**, 2256-2266.
40. Y. Zhu, C. Zeng, T. Chu, H. Wang, Y. Yang, Y. Tong, C. Su and W. Wong, *J. Mater. Chem. A*, 2013, **1**, 11312-11319.
41. Y. Qiu, H. Deng, S. Yang, J. Mou, C. Daiguebonne, N. Kerbellec, O. Guillou and S. R. Batten, *Inorg. Chem.*, 2009, **48**, 3976-3981.
42. L. Pan, K. M. Adams, H. E. Hernandez, X. Wang, C. Zheng, Y. Hattori and K. Kaneko, *J. Am. Chem. Soc.*, 2003, **125**, 3062-3067.
43. S. Ma, D. Yuan, X. Wang and H. Zhou, *Inorg. Chem.*, 2009, **48**, 2072-2077.
44. L. Liu, X. Zhang, Z. Han, M. Gao, X. Cao and S. Wang, *J. Mater. Chem. A*, 2015, **3**, 14157-14164.
45. H. He, D. Yuan, H. Ma, D. Sun, G. Zhang and H. Zhou, *Inorg. Chem.*, 2010, **49**, 7605-7607.
46. J. Heine and K. Muller-Buschbaum, *Chem. Soc. Rev.*, 2013, **42**, 9232-9242.
47. P. Padhye and P. Poddar, *J. Mater. Chem. A*, 2014, **2**, 19189-19200.
48. N. Arshad, N. Abbas, M. H. Bhatti, N. Rashid, M. N. Tahir, S. Saleem and B. Mirza, *J. Photoch. Photobio. B.*, 2012, **117**, 228-239.
49. S. GómezRuiz, B. Gallego, M. R. Kaluđerović, H. Kommera, E. HeyHawkins, R. Paschke and G. N. Kaluđerović, *J. Organomet. Chem.*, 2009, **694**, 2191-2197.
50. G. N. Kaluđerović, H. Kommera, E. HeyHawkins, R. Paschke and S. GómezRuiz, *Metallomics*, 2010, **2**, 419-428.
51. N. Barooah, A. Karmakar, R. J. Sarma and J. B. Baruah, *Inorg. Chem. Commun.*, 2006, **9**, 1251-1254.
52. A. Enzmann, M. Eckert, W. Ponikwar, K. Polborn, S. Schneiderbauer, M. Beller and W. Beck, *Eur. J. Inorg. Chem.*, 2004, **2004**, 1330-1340.
53. S. E. Amos, G. G. Moore, K. E. Nielsen and M. A. Wicki, *Patent*, 2000, **U.S.**, 6096911.
54. G. M. Sheldrick, *Program for X-ray Crystal Structure Refinement, University of Gottingen, Gottingen, Germany*, 1997.
55. J. Song, C. Lei and J. Mao, *Inorg. Chem.*, 2004, **43**, 5630-5634.
56. N. Xu, W. Shi, D. Liao, S. Yan and P. Cheng, *Inorg. Chem.*, 2008, **47**, 8748-8756.
57. Y. T. Yang, C. Z. Tu, H. J. Yin and F. X. Cheng, *Inorganic Chemistry Communications*, 2014, **46**, 107-109.
58. Bu, G. B. Deacon, M. Hilder, P. C. Junk, U. H. Kynast, W. W. Lee and D. R. Turner, *CrystEngComm*, 2007, **9**, 394-411.
59. G. B. Deacon, S. Hein, P. C. Junk, T. Justel, W. Lee and D. R. Turner, *CrystEngComm*, 2007, **9**, 1110-1123.
60. X. H. Miao, S. D. Han, S. J. Liu and X. H. Bu, *Chinese Chemical Letters*, 2014, **25**, 829-834.
61. Y. S. Song and B. Yan, *Inorganica Chimica Acta*, 2005, **358**, 191-195.
62. T. L. Hu, R. Q. Zou, J. R. Li and X. H. Bu, *Dalton Transactions*, 2008, DOI: 10.1039/B716398C, 1302-1311.
63. H. W. Roesky and M. Andruh, *Coordin. Chem. Rev.*, 2003, **236**, 91-119.
64. N. Wei, M. Zhang, X. Zhang, G. Li, X. Zhang and Z. Han, *Cryst. Growth Des.*, 2014, **14**, 3002-3009.
65. E. Assouline, A. Lustiger, A. H. Barber, C. A. Cooper, E. Klein, E. Wachtel and H. D. Wagner, *J. Polym. Sci. Pol. Phys.*, 2003, **41**, 520-527.
66. Z. Li, W. Yang, L. Li, B. Xie, R. Huang and M. Yang, *J. Polym. Sci. Pol. Phys.*, 2004, **42**, 374-385.
67. M. Kristiansen, M. Werner, T. Tervoort, P. Smith, M. Blomenhofer and H.-W. Schmidt, *Macromolecules*, 2003, **36**, 5150-5156.
68. K. Bernland, T. Tervoort and P. Smith, *Polymer*, 2009, **50**, 2460-2464.
69. Z. Wei, W. Zhang, G. Chen, J. Liang, S. Yang, P. Wang and L. Liu, *J Therm Anal Calorim*, 2010, **102**, 775-783.
70. H. Bai, Y. Wang, L. Liu, J. Zhang and L. Han, *J. Polym. Sci. Pol. Phys.*, 2008, **46**, 1853-1867.

Table of Contents
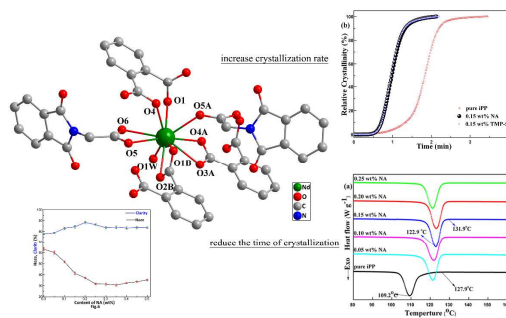
The coordination polymer can increase the overall crystallization rate and a decrease the spherulite size of iPP.